Collisional interference in the foreign-gas-perturbed far-infrared rotational spectrum of HD

P. G. Drakopoulos and G. C. Tabisz
Department of Physics, University of Manitoba, Winnipeg, Manitoba, Canada R3T 2N2
(Received 22 June 1987)

The rotational transitions $R(1)$, $R(2)$, and $R(3)$ of HD have been studied in absorption with 0.06-cm^{-1} resolution in mixtures of HD with He, Ne, Ar, Kr, Xe, H_2, and N_2 at 295 K and at densities between 3 and 62 amagat. Collisional interference was observed and the interference parameter, proportional to the ratio of the average induced moment to the allowed moment, showed a dependence on system size and ranged from $+10\times10^{-3}$ $amagat^{-1}$ for light perturbers to -24×10^{-3} $amagat^{-1}$ for the heavier ones. These interference effects in the pure rotational band are an order of magnitude smaller than those of the fundamental vibrational band and show a strong J dependence not predicted within current theory. The sign of the isotropic overlap component of the induced moment was determined experimentally in an unambiguous way and its trend was found to be within theoretical expectation; specifically, the sign changes as the mass increases. The line shapes were mostly symmetrical and Lorentzian; asymmetry was observed mainly for the $R(1)$ transition with the low-frequency side of the lines super-Lorentzian and the high-frequency side sub-Lorentzian. Investigation of the effect of collision duration on the autocorrelation function of the allowed moment showed it was not important to the integrated allowed absorption.

I. INTRODUCTION

In this paper, a study of the far-infrared rotational spectrum of HD perturbed by a number of foreign gases is reported. The motivation behind this series of experiments is to provide a systematic approach to the study of the collisional interference between allowed and collision-induced transitions, an effect already clearly identified in the HD infrared spectrum.[1–5] The present work is an attempt to settle the controversy regarding the magnitude of the interference in the pure rotational band.[5] The first paper in this series,[6] hereafter referred to as I, reviewed the relevant existing theory on the effect, presented new results for pure HD, and made comparisons with other experiments. The present paper is concerned with experiments in which the inert gases He, Ne, Ar, Kr, and Xe and the diatomic molecules H_2 and N_2 are employed as perturbers. The mixtures with atoms are particularly enlightening in that atoms lack internal vibrational and rotational degrees of freedom and the spectra are more amenable to analysis.

Details of the experiment are discussed in Sec. II. In Sec. III the problems of the analysis are reviewed and data are presented which characterize the behavior of the interference effect, linewidth, and frequency shift for the transitions $R(1)$, $R(2)$, and $R(3)$. Calculation of the interference parameter by available theory is given in Sec. IV. Next follows a discussion of the sign and magnitude of the interference parameter (Sec. V). It is known that the time of duration of collision also modifies the intensity and shape of allowed lines. The role of this mechanism on the observed spectral lines is assessed in Sec. VI.

II. EXPERIMENTAL DETAILS

The experimental techniques and procedure were essentially as described in I. Some additional comment is, however, required. The perturber gases were of the following purity by volume: He, Ne, Ar, and N_2 (99.999%), Kr and Xe (99.995%), and H_2 (99.9995%). The density of HD was held constant at about 10 amagat and the perturber density was varied over the following ranges (in units of amagat): He (6–57), Ne (3–62), Ar (3–48), Kr (3–23), Xe (4–34), N_2 (3–58), and H_2 (3–59). All experiments were performed at 295 K. The densities of the mixtures were determined from equations of state which included the second virial coefficient of the mixture

$$B=\gamma_1^2B_{11}+2\gamma_1\gamma_2B_{12}+\gamma_2^2B_{22}\ ,$$

where γ_1 and γ_2 represent the fractional concentrations of the two species, B_{11} and B_{22} are the second virial coefficients of two species, and B_{12} is the interaction virial coefficient. The fractional concentrations were not known in advance and an iterative procedure was used to estimate them. Virial data were obtained from Dymond and Smith,[7] except for HD-Kr where B_{12} was calculated from the intermolecular potential.

As discussed in I, water lines in the data were usually eliminated in the process of taking the ratio of background and absorption spectra to obtain the absorption coefficient. For some cases, however, notably the $R(1)$ line of HD-He and HD-Ar, water contamination in the sample itself was responsible for absorption features which were not removed by this process. Unlike the pure HD experiments where the sample bottle could be immersed in liquid nitrogen to trap water impurities, here the possibility of a reverse flow of the gas from the cell to the bottle did not permit such a procedure. As a result, lines due to absorption by water were more of a problem and sometimes had to be corrected numerically. In these situations, a Lorentzian was fitted to the water line. Initial parameters were estimated and varied

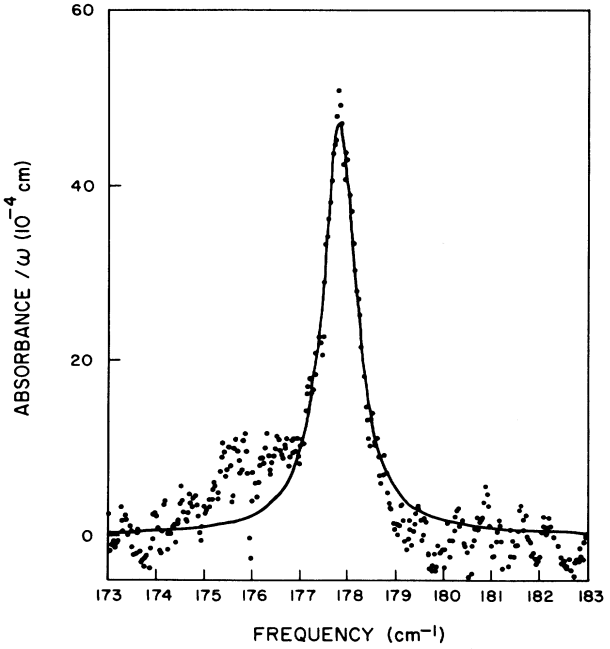

FIG. 1. Ratio of absorbance to frequency for the $R(1)$ line of HD-He at 25.5 amagat. Absorbance is $\log_{10}[I_0(\omega)/I(\omega)]$. Points are experimental. Solid line is the fitted profile [Eq. (9) of I]. Resolution: 0.06 cm^{-1}.

manually for an optimum visual fit. This was followed by application of the simplex method[8] which minimized the rms error between the fitted and experimental spectra. With these estimated parameters, the water lines were then subtracted numerically from the whole spectral region of interest.

III. ANALYSIS OF DATA

The spectral data were analyzed according to the procedure described in Sec. IV of I. The broad collision-induced background was removed. The line-shape function fitted to the data was the sum of a Lorentzian and a dispersion curve [Eq. (9) in I]. Careful observation of the profile revealed some asymmetry of the $R(1)$ line for He, Kr, and Ar mixtures. Nevertheless, the fitting algorithms returned large positive values of q, the asymmetry parameter, which correspond to a Lorentzian profile. Examples of the experimental results and fitted profiles are shown in Figs. 1–4.

The integrated absorption coefficients were then determined analytically [Eq. (11) in I] and plotted versus density (Figs. 5 and 6). These can be expressed in powers of the density through Eq. (12) in I:

$$\int [\alpha(\omega)/\rho_a N_0 \omega] d\omega = c_0 + c_1 \rho + c_2 \rho^2 .$$

The density ρ_a is that of the absorber and ρ is that of the perturber; $\alpha(\omega)$ is the absorption coefficient at frequency ω; N_0 is Loschmidt's number. The coefficients c_0, c_1, and c_2 were determined. In the theory of collisional interference,[3,9] a, the interference parameter, is given as

$$a = \frac{c_1}{c_0} = 8\pi N_0 \Delta' \frac{\int_0^\infty \langle J \mid p^I(R) \mid J' \rangle g(R) R^2 dR}{\langle J \mid p^A \mid J' \rangle} .$$

Here $p^I(R)$ is the component of the induced moment which has the appropriate symmetry to permit interference with transitions involving the allowed moment p^A; $g(R)$ is the pair distribution function, Δ' is a phase factor, and R is the intermolecular distance. The rotational

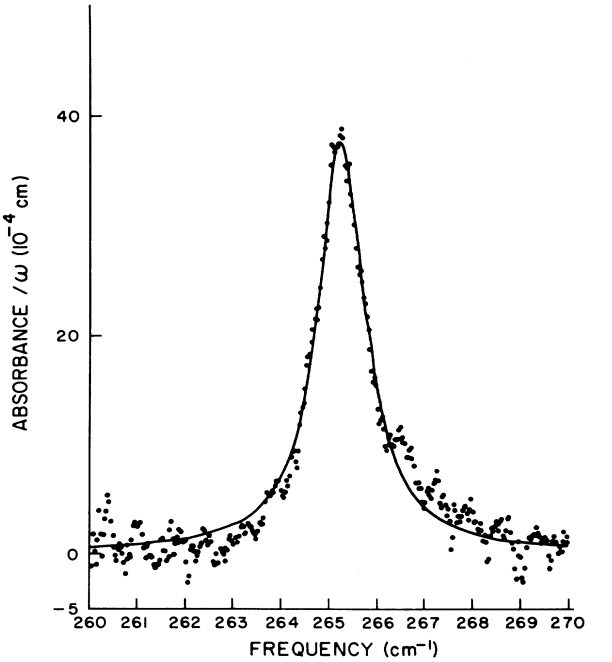

FIG. 2. Ratio of absorbance to frequency for the $R(2)$ line of HD-Ne at 56.2 amagat. Points are experimental. Solid line is the fitted profile [Eq. (9) of I]. Resolution: 0.06 cm^{-1}.

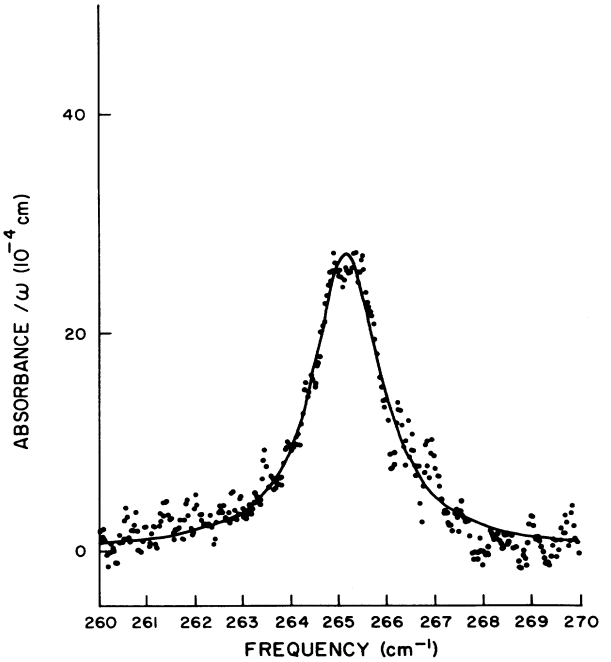

FIG. 3. Ratio of absorbance to frequency for the $R(2)$ line of HD-Ar at 69.5 amagat. Points are experimental. Solid line is the fitted profile [Eq. (9) of I]. Resolution: 0.06 cm^{-1}.

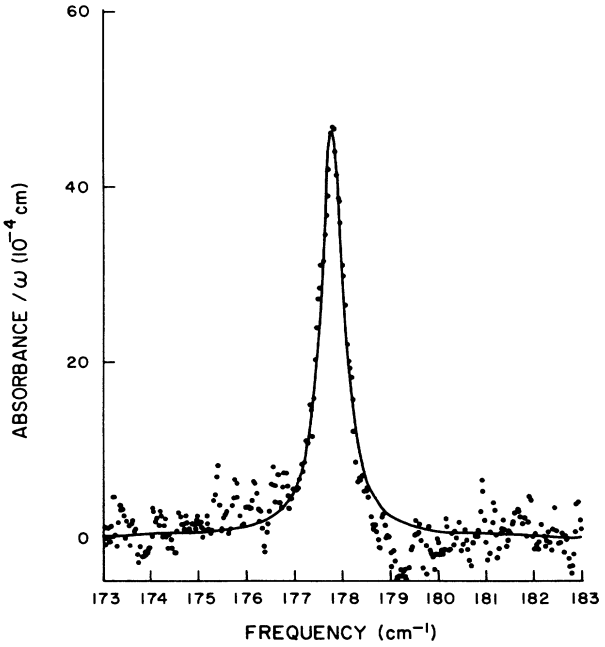

FIG. 4. Ratio of absorbance to frequency for the $R(1)$ line of HD-Xe at 7.0 amagat. Points are experimental. Solid line is the fitted profile [Eq. (9) of I]. Resolution: 0.06 cm^{-1}.

quantum numbers J and J' are those of the initial and final states of the transition. The interference parameter is thus proportional to the ratio of the average induced moment to the allowed moment. The meaning of a is more fully explained in I. The values of a found are given in Table I.

The broadening coefficient B_0 and frequency shift coefficient S_0 were obtained through Eqs. (16) and (17) in I and are listed in Tables II and III, respectively:

$$\gamma = B_0\rho + K_1 ,$$

$$\omega_0 = S_0\rho + \omega_0^0 .$$

The full width at half height of the line is γ, peak frequency is ω_0, zero-density frequency is ω_0^0, and K_1 is a constant.

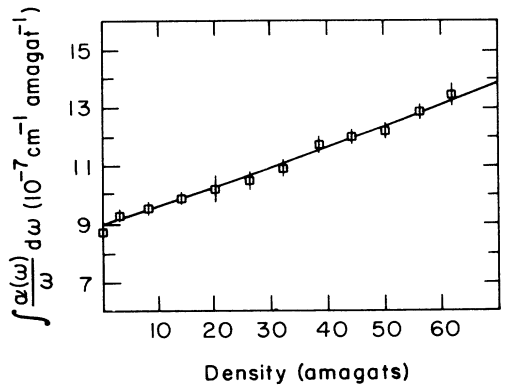

FIG. 5. Integrated absorption coefficient of $R(2)$ for HD-Ne as a function of density. Points are experimental. Solid line is the fitted curve [Eq. (12) of I, method (c)].

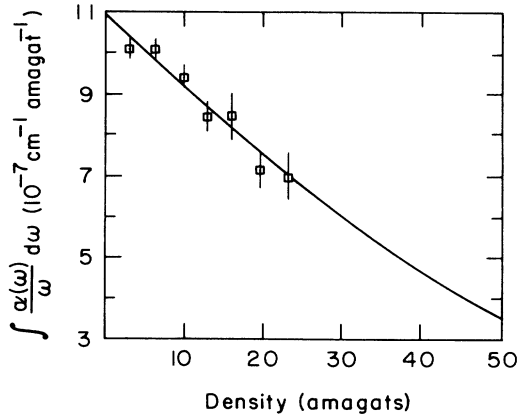

FIG. 6. Integrated absorption coefficient of $R(1)$ for HD-Kr as a function of density. Points are experimental. Solid line is the fitted curve [Eq. (12) of I, method (c)].

The errors shown in the tables represent the statistical uncertainty (1σ) in the displayed quantity as deduced from the weighted fitting procedure. Both positive and negative values of the parameter a appear, corresponding to constructive and destructive interference. The broadening coefficients generally decrease with increasing J. The shifts of frequency with increasing density are blue for $R(1)$ and $R(2)$, with the exceptions of $R(2)$ of Kr and Xe. The fact that essentially symmetric profiles were fitted to the experimental results, even though some slight asymmetry is visually evident, has a minimal effect on the integrated absorption and linewidths but does have implications for the deduced line shifts. A frequency shift other than that predicted by pressure broadening theory is introduced when, in order to accommodate asymmetry, a dispersion curve is part of the fitted profile [Eq. (9) in I].

The remarks on the quality of the data given in Sec. IV of I apply here as well. Experimental conditions varied somewhat for each mixture studied. As a result, the quality on the spectra is thought to decrease in the following order: Ne, Kr, Xe, He, H_2, Ar, and N_2. Again, as for pure HD the order of quality among the lines is $R(2)$, $R(1)$, and $R(3)$. This assessment should be kept in mind through the remaining discussion where all mixtures are treated essentially on an equal basis.

TABLE I. Experimental interference parameter a (10^{-3} $amagat^{-1}$).

Perturber	$R(1)$	$R(2)$	$R(3)$
He	+5.7(9)	+3.9(8)	+10.0(19)
Ne	+2.1(4)	+6.9(4)	+5.3(12)
Ar	+1.8(3)	+6.1(2)	+9.4(11)
Kr	−17.4(24)	−4.3(36)	−6.7(59)
Xe	−23.9(19)	−10.0(23)	−8.2(44)
HD	−1.1(2)	+1.3(1)	+2.1(6)
H_2	−2.4(5)	−0.9(3)	+4.3(18)
N_2	−10.8(12)	+6.1(7)	+4.6(21)

TABLE II. Broadening coefficient B_0 (10^{-2} cm^{-1} amagat^{-1}).

Perturber	$R(1)$	$R(2)$	$R(3)$
He	2.13(6)	1.35(4)	1.17(9)
Ne	1.68(3)	1.50(2)	0.68(6)
Ar	2.96(4)	2.19(2)	1.35(5)
Kr	2.16(14)	2.11(21)	0.46(22)
Xe	3.89(15)	2.29(16)	0.82(18)
HD	2.53(1)	2.20(1)	1.81(3)
H_2	2.66(5)	2.10(3)	1.66(13)
N_2	2.41(13)	2.62(6)	1.33(13)

TABLE III. Frequency shift coefficient S_0 (10^{-3} cm^{-1} amagat^{-1}).

Perturber	$R(1)$	$R(2)$	$R(3)$
He	+ 2.4(2)	+ 2.8(1)	+ 1.8(3)
Ne	+ 4.4(1)	+ 2.4(1)	+ 0.3(2)
Ar	+ 8.3(3)	+ 1.3(1)	− 1.1(2)
Kr	+ 4.6(4)	− 0.5(7)	− 1.3(9)
Xe	+ 3.8(6)	− 3.6(5)	− 3.8(6)
HD	+ 0.6(1)	+ 0.6(1)	− 0.4(1)
H_2	+ 0.1(2)	+ 0.2(1)	− 0.6(5)
N_2	+ 7.0(4)	+ 1.5(2)	+ 0.4(4)

IV. CALCULATION OF INTERFERENCE PARAMETERS

The necessary information exists in the literature for the calculation of the interference parameter a for He, Ar, Kr, and Xe mixtures following the method of I, Sec. IV. For H_2-He and H_2-Ar, Meyer and Frommhold[10] have performed *ab initio* calculations of the overlap dipole moments and give their results in the form of Eq. (19) in I. The parameters they obtain are accurate to about 5% (Table IV). For H_2-Kr and H_2-Xe, semiempirical moment strengths determined by Poll and Hunt[11] were available. Their parameters have about 10% accuracy (Table IV). For the intermolecular potentials, both an *ab initio* form[12] (HD-He) and a Buckingham-Corner semiempirical expression[13] (HD-Ar, HD-Kr, HD-Xe) were employed.[13] The H_2-X dipole moment functions were made applicable to the HD-X case by shifting the origin from the molecular midpoint to the HD center of mass with the use of Eq. (5) in I. As well, the H_2-X potentials appearing in the literature[12,13] were transformed to the HD-X system by Eq. (22) in I. The interference parameters were obtained through Eqs. (18)–(23) in I. For the cases of mixtures, both $[A_1(100)]_0$ and $[A_1(100)]_2$ contribute to the induced moment matrix elements. Unfortunately for the Kr and Xe mixtures only the isotropic overlap moment component $A_0(001)$ was known and thus only $[A_1(100)]_0$ could be calculated. Rotational level mixing corrections[14] to the interference parameter designated by Δa were estimated for HD-Ar and HD-He.

The results of these calculations are presented in Table V. The positive sign of a for He and Ar mixtures was deduced as explained in Sec. V A. The question marks indicate that the sign of a could not be calculated for the other mixtures. The correction Δa is always added to a so as to increase its magnitude.

V. DISCUSSION

A. Comparison with the theory of interference

Since the interference effects could be calculated for only five systems, namely HD-He, HD-HD (H_2), HD-Ar, HD-Kr, and HD-Xe and since, moreover, for the last two systems, only isotropic overlap contributions are taken into account, a full comparison of experiment and theory is not possible. Nevertheless, a general comparison and trend identification will be attempted here.

The experimental values of a (Table I) for pure HD and the inert gas mixtures are plotted along with the theoretical calculations (Table V) in Fig. 7 as a function of the perturber polarizability. This polarizability was chosen as the most appropriate variable since the overlap induced moment is expected to be roughly propor-

TABLE IV. Overlap-induced moment parameters.

Perturber	$A^{(7)}$ (D Å^{-7})	$A^{(0)}$ (10^{-3} D)	b_1 (Å^{-1})	b_2 (Å^{-2})	σ (Å)
			$A_0(001)$		
He	−2.383	6.358	−3.161	−0.161	3.015
Ar	−8.205	8.488	−3.569	−0.336	3.174
Kr		16	−2.754		3.301
Xe		17	−2.583		3.520
			$A_2(201)$		
He		−0.911	−3.200	−0.039	3.015
HD		1.659	−3.180		3.019
Ar		−3.814	−2.977	0.114	3.174

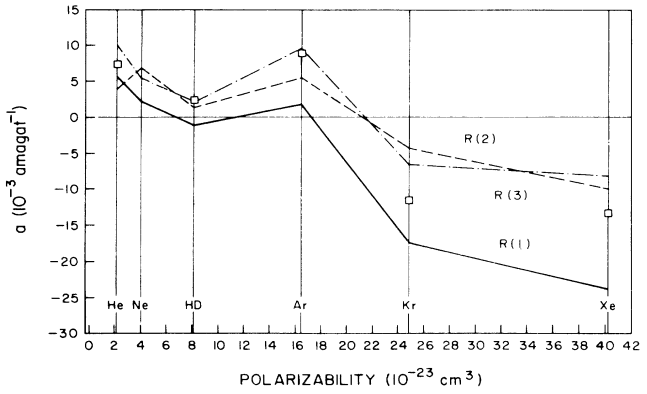

FIG. 7. The experimental and calculated interference parameter a for pure HD and HD-inert gas mixtures as a function of perturber polarizability. Experimental: $R(1)$ (——); $R(2)$ (— — —); $R(3)$ (—·—·—·). Calculated: □.

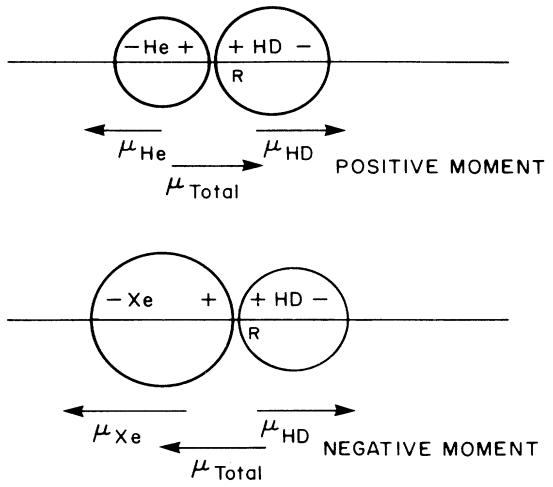

FIG. 8. Pictorial representation of the overlap-induced moment generation for two extreme systems: HD-He and HD-Xe.

tional to it.

The first striking trend is the tendency for a to decrease, roughly inversely proportional to the polarizability; moreover, the sign changes at some point. These results can be understood as follows.

1. Sign of the induced moment

The sign of the interference depends on the relative orientation of the allowed transition moment and the $A_1(100)$ component of the induced moment. Both moments lie along the internuclear axis of the HD molecule. The allowed moment has always a direction H^+D^-, and therefore the sign of interference will depend on which direction the overlap component points. According to the coordinate system and notation established in Figs. 1 and 2 of I, a positive overlap component $A_0(001)$, which points from the perturber to the HD molecule (for example He^+HD^-), will give a shifted moment component $A_1(100)$ which points from hydrogen to deuterium. This results in positive interference. For the anisotropic overlap $A_1(201)$, the opposite is true; when it is negative, rather than positive, the resulting interference is positive. The sign of overlap components which were obtained by inversion of CIA (collision-induced absorption) spectra[11] (HD-Xe and HD-Kr) cannot be specified since the square of the dipole moment is responsible for the spectrum. On the other hand, *ab initio* calculations supply the direction of the induced moment. According to Ref. 10, for both HD-He and HD-Ar the $A_0(001)$ overlap component is positive and therefore the collisional allowed-induced interference should be positive. No information is given, however, in Ref. 10 about the sign of the anisotropic overlap component of H_2-H_2 where the perturber and the active molecule are the same species.

The simplified pictorial simulation in Fig. 8 gives a qualitative explanation of why the induced moment can change direction from system to system. The overlap or exchange induced moment originates at short intermolecular distances as a result of the exclusion principle. During the collision, the electronic cloud of the outer orbital of each molecule is pushed outwards when the two electronic clouds are brought into contact. This interaction induces a net moment on each molecule. If the two molecules differ, a pair moment appear which is the algebraic sum of the two moments. Therefore, the short ranges forces generally give a moment with the more polarizable molecule (or atom) negative since it suffers the most distortion. Then one expects that molecules much lighter than HD will give positive collisional interference, whereas, those much heavier than hydrogen molecules (higher polarizability) will give negative interference. Indeed, in general, this is the trend in the data and can easily be seen in Table I.

Since it is expected that the $R(3)$ line will be less sensitive to effects due to the anisotropic part of the potential,[3,14] the sign of the theoretical a, where it cannot be

TABLE V. Calculated interference parameter (10^{-3} amagat^{-1}).

		Δa			
Perturber	a	$R(0)$	$R(1)$	$R(2)$	$R(3)$
He	+7.3	0.2	0.2	0.1	0.2
Ar	+8.9	1.0	1.1	0.6	1.3
Kr	?11.6				
Xe	?13.4				
HD	?2.3	0.8	0.9	0.3	0.9
H_2	?2.2	0.8	0.9	0.3	0.9

calculated, is chosen such that it follows the pattern of the measured sign for $R(3)$. The individual points that appear in Fig. 7 represent the calculated a.

An important result of this work, therefore, is the experimental determination of the sign of the overlap, induced-moment component for various mixtures of HD. This information clearly cannot be deduced from ordinary collision-induced spectroscopy.

2. *Magnitude of a*

Now that the overall trends are established, a direct comparison of theory and experiment for individual lines can follow. First, there is good agreement for the case of pure HD, particularly for the $R(2)$ and $R(3)$ lines. For the other systems there is less overall agreement but still it is better for the $R(2)$ and $R(3)$ lines. It is apparent in Fig. 7 that the interference effects in $R(1)$ are stronger than for the other lines. This effect implies that there is an additional subtractive contribution to the $R(1)$ interference term. Possible reasons for this can be the following.

(i) An additional term $2\langle p^I(R)\rangle/p^A(r)$ is added due to anisotropic interactions that mix the rotational states. However, in the only treatment of this effect to date,[14] the magnitude of the additional interference Δa (Table V) does not explain such a discrepancy for the $R(1)$ data.

(ii) The induced moment has a J dependence. However, according to Ref. 3, the matrix elements $\langle J' \mid p^I(r,R) \mid J \rangle$ are found to have a negligible J dependence. Moreover, in the *ab initio* calculations of Meyer and Frommhold,[10] it is shown that the induced moment increases as r increases; r is the internuclear distance in HD. Therefore larger interference effects are expected in higher J lines. On the other hand, the collisional cross section of the $R(1)$ transition is larger than the $R(2)$ and $R(3)$ and this might have an effect on the average induced moment.

(iii) The allowed moment changes magnitude. In the *ab initio* estimations of this moment such behavior is not predicted. However, there is always the possibility that the mixing of the states will modify the matrix elements of the allowed moment (although this effect will be of second order[3]).

(iv) There is a systematic error. The $R(1)$ line of the mixtures has a large broadening coefficient compared to $R(2)$ and $R(3)$ and, as a consequence, in the analysis procedure the base-line determination becomes much more difficult. This argument, however, contradicts the fact that a larger line asymmetry was observed for the $R(1)$ transition, which implies that the observed larger interference effect must be real.

Comparison of Eqs. (8) and (18) of I shows that the phase shift Δ' can also be estimated simply by dividing the experimental a by the theoretical a and by assuming that Δ' is the only factor that contributes to the discrepancy of the two. For $R(2)$ the values range from 0.75 to 0.53, but for $R(1)$ they exceed unity which is not realistic.[9] This is an additional indication that there exist more effects than the Δ coefficient introduces.

In Table V the interference contributions Δa generated from the mixing of the rotational states are compared to the theoretical value of a. This mechanism always increases the absolute value of the interference. The contribution has a small effect and it is difficult to detect whether any change results in the agreement between theory and experiment by addition of Δa to $\mid a \mid$.

Finally, an interesting result is that the HD-H_2 system revealed stronger interference effects than the pure HD for $R(1)$ and $R(3)$.

3. *Comparison with fundamental band*

The interference parameters a found in this work for the rotational band are about an order of magnitude less than those reported[3,15] for the fundamental vibration-rotation band. This is to be expected as the matrix elements of the allowed moment p^A are about an order of magnitude greater for 0-0 transitions than for 1-0 transitions[16] and a is inversely proportional to these elements. Moreover, for pure HD only the anisotropic component of the overlap moment contributes to the interference, while both the isotropic and anisotropic components participate in the interference effect for the fundamental band and the interference parameter depends directly on these components.

The elements of p^A for the rotational band are negative (H^+D^-), while they are positive (H^-D^+) for the fundamental band.[16] For the pair HD-He the component of the overlap induced moment along the internuclear axis of HD is positive (H^+D^-). Thus for the fundamental band, a is calculated to be negative. Indeed, McKellar and Rich[15] observe a to be negative for HD-He, HD-Ne, and HD-Ar. Poll *et al.*[2] find a to be positive for HD-Kr. Thus there is a change of sign for the heavier perturbers. Therefore the same trends on a are found for the rotational and fundamental bands with the difference in sign due to the opposite signs of the allowed moment elements.

B. Further observations

1. *Line asymmetry*

The line asymmetry observed is definitely not as large as observed in the vibration-rotation region.[9] In all the present cases, any asymmetry appeared on the $R(1)$ line only. With the light perturbers, especially He (Fig. 1), the low-frequency side of the line was higher in intensity (super-Lorentzian). For the heavy perturbers, Kr and Xe (Fig. 4), there is a dip in intensity on the high-frequency side (sub-Lorentzian) suggestive of the presence of a dispersion component. It seems to disappear at the highest densities studied for Xe.

Large line asymmetry was observed with smaller mass perturbers, even though there exists a substantial negative frequency shift for the heavier perturbers. Herman[17] explains this observation to be a result of the fact that the predominantly red-shifting collisions are matched by the less numerous blue-shifting collisions, when weighted by the induced dipole magnitude.

2. *Shift of the collision-induced spectrum*

A large blue shift, over 10 cm^{-1}, of the peak of the collision-induced $S_0(0)$ line was observed (see Fig. 9). This shift was previously observed in the CIA spectrum of H_2 and was attributed to the quantum character of the line.[18] However, HD additionally possesses the allowed rotational spectrum, which has a negligible relative shift, and this phenomenon is more effectively demonstrated here.

3. *Impact approximation*

For the broadening and shift coefficients, it can be verified that the general tendency of the results follows the trends of the impact approximation. The widths and the shifts are proportional to the real and imaginary parts of the collision cross section, respectively. Although the computation of this cross section is beyond the scope of this work, from study of calculations of similar systems, the trends can be established; for the pure rotational band, the cross section usually decreases as the quantum number J or the perturber size increases and the negative (blue) shift increases with J or the perturber mass.[19,20]

VI. TIME OF DURATION

The quantitative agreement of the theoretical and experimental intensity is not fully satisfactory, especially for $R(1)$. This indicates that additional mechanisms affect the absorption lines at medium densities. Such a mechanism, other than the collisional interference, which is capable of modifying the intensity of the spectral lines, involves the effect of duration of the collisions. In this section, the magnitude of this contribution to the modification of the rotational lines will be estimated.

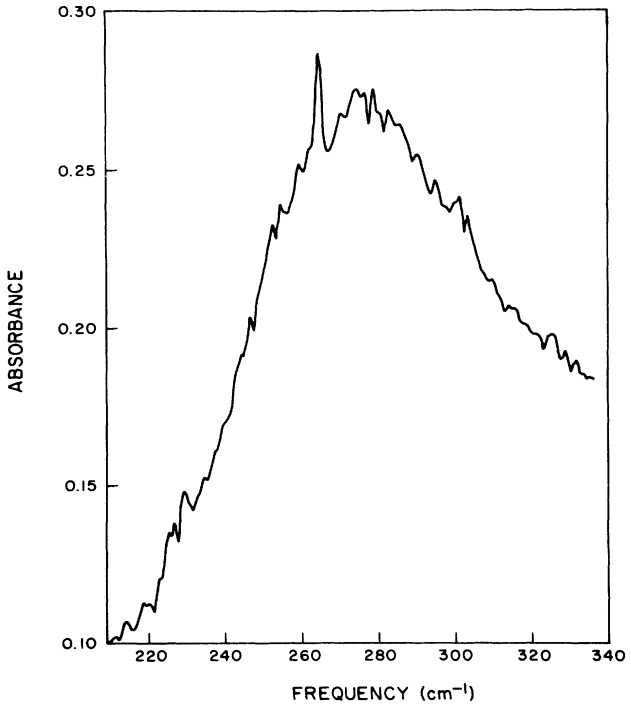

FIG. 9. The $R(2)$ region for HD-Xe at 34 amagat. The sharp $R(2)$ line is at about 265 cm^{-1}, while the peak of the broad $S_0(0)$ line is displaced to higher frequencies.

When the autocorrelation function of the allowed dipole moment was evaluated in I, the assumption was made that the time of the duration of the collison was negligible compared to the time between collisions. This corresponds to the so-called impact approximation.

In general, the correlation function will be proportional to

$$\exp(i\omega_0^0 t)\langle\langle JJ' \mid \langle U^{-1}(t)\rangle \mid JJ'\rangle\rangle \ , \tag{1}$$

where U^{-1} is the evolution operator in the Liouville representation.[21] Under some assumptions,[22] the matrix elements that appear in (1) can be put in the form

$$\langle\langle JJ' \mid \langle U^{-1}(t)\rangle \mid JJ'\rangle\rangle = \exp[-nh(t)] \ , \tag{2}$$

where n is the number density.

In the impact approximation, the behavior of $h(t)$ has the familiar linear form

$$h(t) = n^{-1}(\gamma + i\delta)t/2 \tag{3}$$

with $\gamma/2$ and $\delta/2$ as the pressure-broadened half width at half maximum (HWHM) and line shift, respectively. However, if the time of collision duration τ is taken into account, the asymptotic behavior of $h(t)$, for $t \gg \tau$, is of the form[23]

$$h(t \gg \tau) = n^{-1}[(\gamma + i\delta)(t/2) + a' + ib'] \ . \tag{4}$$

If $h(t)$ is approximated by this asymptotic expression, the Fourier transform of the autocorrelation function gives a modification of the line shape [Eq. (2) of I],

$$\begin{aligned}\phi(\omega) = {} & |\langle J \mid p^A(r) \mid J'\rangle|^2 (J+1)P(J) \\ & \times \{\exp(-a')(\gamma/2\pi)/[(\gamma/2)^2 + (\omega-\omega_0)^2] \\ & + \exp(-a')(b'/\pi)(\omega-\omega_0)/[(\gamma/2)^2 \\ & + (\omega-\omega_0)^2]\} \ ,\end{aligned} \tag{5}$$

where again $\omega_0 = \omega_0^0 + \delta/2$ (shifted line position). Since a' is a small quantity, by expanding the term $\exp(-a')$ to the first order, (5) becomes

$$\begin{aligned}\phi(\omega) = {} & |\langle J \mid p^A(r) \mid J'\rangle|^2 (J+1)P(J) \\ & \times \{(1-a')(\gamma/2\pi)/[(\gamma/2)^2 + (\omega-\omega_0)^2] \\ & + (1-a')(b'/\pi)(\omega-\omega_0)/[(\gamma/2)^2 \\ & + (\omega-\omega_0)^2]\} \ .\end{aligned} \tag{6}$$

This spectral profile would be valid for a range of densities such that $\gamma \pi c \tau < 1$, i.e., lower than 100 amagat. Clearly this line shape is asymmetric due to the presence of the dispersion term. Moreover, the intensity is modified by a factor a'. A positive a' corresponds to a

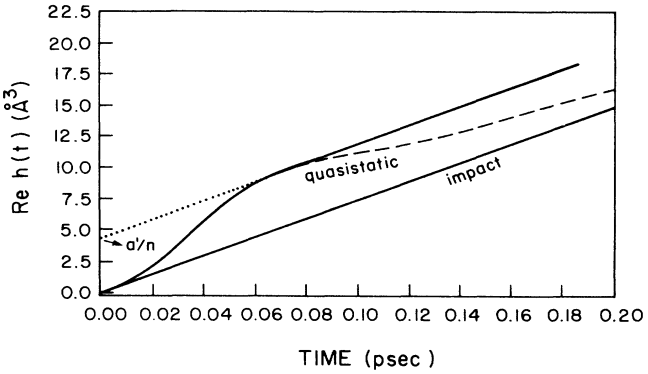

FIG. 10. Calculated synthesized function $h(t)$ for the $R(2)$ line of HD-Kr.

reduction in the total intensity. Thus, if the asymptotic behavior of the real part of $h(t)$ for $t \gg \tau$ is known, then by extrapolation to $t=0$, the asymmetry factor a'/n and the effect on the intensity can be estimated.

It is interesting to note that this line shape is similar to the Fano type predicted by the interference theory, i.e., a superposition of a Lorentzian and a dispersion contour, Eq. (6) of I. Thus the time of duration contribution produces changes in intensity and line profile similar to the interference effect. The parameter $-a'$ plays the same role in this formalism as does $+a\rho$ in the theory of collisional interference.

Usually the function $h(t)$ can be obtained through two separate approaches. For times smaller than the duration of collision τ, the quasistatic approximation gives accurate results. For times much larger than τ the impact limit is adequate. Those two limiting approaches can be then unified (synthesized) to obtain a convenient representation of the $h(t)$ function accurate in the intermediate regime between the quasistatic and the impact one.[24]

In the quasistatic approximation, and for the pure rotational lines, the treatment of Boulet *et al.*[24] gives $h(t)$ as

$$h(t)=4\pi \int_0^\infty \left[1-\exp\left[-\sum_l Q_l(R,t)\right]\right] R^2 \times \exp[-V_0(R)]dR \quad (7)$$

with

$$Q_l(R,t)=[1/(2l+1)][V_l(R)t/(2\hbar)]^2 C(t) \ . \quad (8)$$

The parameter l denotes the order of the Legendre polynomial in the expansion of the anisotropic interaction potential $V_l(R)$; R is the intermolecular distance. $C(t)$, is, in general, a complex function of time and depends on l and the rotational transition frequencies.

For the present problem, collision of HD with a perturber atom, only the first two terms of the potential expansion are kept: the $V_1(R)$ component that arises from the displacement of charge and mass centers (P_1 anisotropy [Eq. (22) of I] and the $V_2(R)$ component that arises from the quadrupole-induced dipole interaction (P_2 anisotropy).

TABLE VI. Time of duration of collision parameter d (10^{-4} amagat^{-1}).

Perturber	$R(1)$	$R(2)$	$R(3)$
Ar	−2.15	−0.70	−0.87
Kr	−2.28	−1.21	−1.53
Xe	−1.49	−1.69	−1.73

Finally, the real part of the impact approximation of $h(t)$, as can be seen from Eq. (3), is simply a straight line with slope equal to the pressure broadened HWHM $\gamma/2$ of the particular rotational line considered.

The problem now is to obtain a representation of the $h(t)$ function in the intermediate regime. From the treatment of Boulet *et al.*,[24] an approximate form can be obtained by a simple translation of the impact straight line in such a way that the impact Re$h(t)$ becomes tangential to the quasistatic Re$h(t)$ function. This procedure is illustrated in Fig. 10. The synthesized function will consist partially of the quasistatic part and partially of the translated impact line.

The example of Fig. 10 was carried out for all HD-atom systems. Although the $V_2(R)$ component of the anisotropy is stronger than $V_1(R)$, its effect on Re$h(t)$ was found negligible and ignored in the final calculations. For the impact approximation of Re$h(t)$, the assumption was made that the observed lines broaden according to the impact theory, and the broadening coefficients of Table II were used. By extrapolation of the translated $h(t)$ to $t=0$, a'/n was obtained. For a direct comparison with the parameter a of the interference theory, it is convenient to introduce the parameter d,

$$d=-a'N_0/n \ . \quad (9)$$

The inclusion of N_0 results in units of amagat^{-1} for d and the negative sign corrects for the sign difference between the two formalisms mentioned above. The results are displayed in Table VI.

It appears that the effects of the time of duration on the permanent dipole moment correlation function are not important compared to the interference effects; d is one to two orders of magnitude smaller than a to which it should be added in order to describe the total charge in intensity. An interesting point is that, for the case of light perturbers, the above graphical approximation was found inadequate for synthesizing the function; at no time was the translated impact line tangent to the quasistatic $h(t)$, except possibly at the origin.

VII. SUMMARY

Collisional interference was observed and the interference parameter, proportional to the ratio of the average induced moment to the allowed moment, showed a dependence on system size and ranged from $+10\times10^{-3}$ amagat^{-1} for light perturbers to -24×10^{-3} for the heavier ones. These interference effects in the pure rotational band are an order of magnitude smaller than those of the fundamental vibrational band and show a strong J

dependence not predicted within current theory. The sign of the isotropic overlap component of the induced moment was determined experimentally in an unambiguous way and its trend was found to be within theoretical expectation; specifically the sign changes as the mass increases. The line shapes were mostly symmetrical and Lorentzian; asymmetry was observed mainly for the $R(1)$ transition with the low-frequency side of the lines super-Lorentzian and the high frequency side sub-Lorentzian. Investigation of the effect of collision duration on the autocorrelation function of the allowed moment showed it was not important to the integrated allowed absorption.

ACKNOWLEDGMENTS

We wish to acknowledge helpful discussions with G. Birnbaum. This work was supported by the Natural Sciences and Engineering Research Council of Canada.

[1]A. R. W. McKellar, Can. J. Phys. **51**, 389 (1973).
[2]J. D. Poll, R. H. Tipping, R. D. G. Prasad, and S. P. Reddy, Phys. Rev. Lett. **36**, 248 (1976).
[3]R. H. Tipping, J. D. Poll, and A. R. W. McKellar, Can. J. Phys. **56**, 75 (1978).
[4]J. B. Nelson and G. C. Tabisz, Phys. Rev. A **28**, 2157 (1983).
[5]A. R. W. McKellar, Can. J. Phys. **64**, 227 (1986).
[6]P. G. Drakopoulos and G. C. Tabisz, preceding paper, Phys. Rev. A **36**, 5556 (1987).
[7]J. H. Dymond and E. B. Smith, *The Virial Coefficients of Pure Gases and Mixtures* (Clarendon, Oxford, 1980).
[8]J. A. Nelder and R. Mead, Comput. J. **7**, 308 (1965).
[9]R. M. Herman, R. H. Tipping, and J. D. Poll, Phys. Rev. A **20**, 2006 (1979).
[10]W. Meyer and L. Frommhold, Phys. Rev. A **34**, 2771 (1986); **35**, 2936 (1986).
[11]J. D. Poll and J. L Hunt, Can. J. Phys. **54**, 461 (1976).
[12]P. E. S. Wormer and G. Van Dijk, J. Chem. Phys. **70**, 5695 (1979); F. Mulder, A. van der Avoird, and P. E. S. Wormer, Mol. Phys. **37**, 159 (1979).
[13]J. P. Toennies, W. Welz, and G. Wolf, J. Chem. Phys. **71**, 614 (1979).
[14]G. C. Tabisz and J. B. Nelson, Phys. Rev. A **31**, 1160 (1985).
[15]A. R. W. McKellar and N. H. Rich, Can. J. Phys. **62**, 1665 (1984).
[16]L. Wolniewicz, Can. J. Phys. **54**, 672 (1976); A. L. Ford and J. C. Browne, Phys. Rev. A **16**, 1992 (1977); W. R. Thorson, J. H. Choi, and S. K. Knudson, *ibid.* **31**, 22 (1985); **31**, 34 (1985).
[17]R. M. Herman, in *Proceedings of the 8th International Conference on Spectral Line Shapes*, edited by R. Exton (Deepale, Hampton, 1987).
[18]G. Birnbaum and E. R. Cohen, Can. J. Phys. **54**, 593 (1976).
[19]Krishnaji and S. L. Srivastava, J. Chem. Phys. **43**, 1345 (1965).
[20]R. H. Tipping and R. H. Herman, J. Quant. Spectrosc. Radiat. Transfer, **16**, 881 (1970); **16**, 897 (1970).
[21]U. Fano, Phys. Rev. **131**, 259 (1963).
[22]D. Frenkel and J. van der Elksen, J. Chem. Phys. **67**, 4243 (1977).
[23]Ph. Marteau, C. Boulet, and D. Robert, J. Chem. Phys. **80**, 3632 (1984).
[24]C. Boulet, D. Robert, and L. Galatry, J. Chem. Phys. **72**, 751 (1980); C. Boulet, and D. Robert, *ibid.* **77**, 4288 (1982).